



Mineralogical and textural arguments for a metasomatic origin of the Ougnat pyrophyllite, Eastern Anti-Atlas, Morocco

A. Essalhi¹, M. Essalhi^{1*}, A. Toummite¹, A. El Mostadi², Y. Raddi³

1 : Equipe de Recherche : Géophysique, Géoressources et Patrimoine (ER-GGP). Département de Géologie, Faculté des Sciences et Techniques, BP 509 Boutalamine, Errachidia. Maroc

2 : Unité de Recherche Associée au CNRST (URAC 45), Département de Géologie, Faculté des Sciences, B.P. 20 - Bd des Facultés – 24000, EL Jadida, Maroc

3 : Direction de la Géologie, Ministère de l'Energie et des Mines, B.P. 6208, Rabat Instituts, Haut Agdal, Rabat, Maroc

Received 15 Jun 2016, Revised 20 Nov 2016, Accepted 23 Nov 2016

*For correspondence: Email: mourad.essalhi@gmail.com

Abstract

The Moroccan Anti-Atlas is rich by different types of mineralization such as precious metals, base metals and industrial minerals like talc, barite and pyrophyllite. At the extreme east of the Anti-Atlas, the Precambrian exhumed anticline of Ougnat contain several indices and deposits of pyrophyllite in the Neoproterozoic volcanic rocks. Two main deposits of the Ougnat inlier were studied: the Isk n'Oudadène and the Boumadine pyrophyllitic deposits. The observation and sampling concerned various evolution stages of the pyrophyllite from the intact rhyolitic protore to the most mature pyrophyllite. The mineralogical and textural analysis of the pyrophyllite and its immediate surrounding rocks shows a metasomatic origin of the pyrophyllite from the rhyolitic protolith. Consequently, the mineralizing fluid induced a change in the overall chemical composition of the original rocks (rhyolite) and allowed the pyrophyllite crystallization in the two studied ore deposits.

Keywords: pyrophyllite, protolith, metasomatism, rhyolite, Ougnat, Iskn'Oudadène, Boumadine.

1. Introduction

Pyrophyllite is a hydrous aluminum phyllosilicate $\text{Al}_2\text{Si}_4\text{O}_{10}(\text{OH})_2$. It gets its name from the Greek words for fire and leaf as in "fire-leaf", from the fact that it exfoliates when water is driven off upon heating, leaving a flaky mass. The flakes are actually the silicate sheets that are a testament to pyrophyllite's structure. With its physicochemical properties, pyrophyllite is an industrial mineral of great economic value. Pyrophyllite is formed by supergene and hydrothermal alteration of igneous rocks and felsic schists derived from metamorphic aluminous volcanic ash, especially rhyolitic lava flow like pyrophyllite deposit of the Avalon Peninsula of Newfoundland [1-4] and Pinite mine in Nevada [5]. The formation of the pyrophyllite involve outward migration of silica and alkalis, leaving behind less mobile alumina [2]; Pyrophyllite is also identical in physical properties to a quite distinct mineral called talc. The two are isomorphous, meaning they share the same monoclinic or triclinic structure but have different chemistries. Talc has magnesium instead of aluminum and is indistinguishable from pyrophyllite without a chemical test for aluminum. Their analogous physico-chemical properties (as chemical inertness, high dielectric strength, high melting point and low electrical conductivity) give their similar industrial uses. Talc and pyrophyllite are from the TOT phyllosilicates group (flake's charge = 0). TOT layers, electrically neutral, are weakly linked by Van der Waals bonds. This gives a perfect cleavage (001), mineral is then easily debited in flakes well-known plates of these minerals (Figure 1).

The main producers of pyrophyllite in the world are South Korea (750 kt) and Japan (370 kt) [7] (Statistics of 2007). In Morocco, many deposits of pyrophyllite are hosted in the Precambrian rocks of the Ougnat inlier

(Eastern Anti-Atlas). Some deposits have already been exploited by open pit like the Isk n'Oudadène and the Boumadine deposits (Figure 2). These two deposits, operated by two Moroccan companies: Zenaga and Ouisselsate-Mine respectively, produced a total of industrial ore exceeding 500000T until 2014.

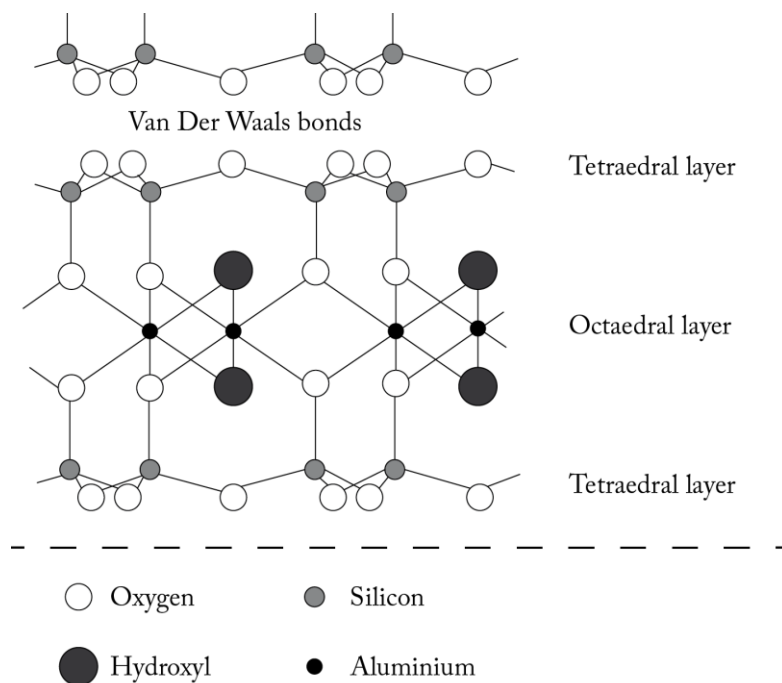


Figure 1: TOT atomic structure of pyrophyllite [6].

The pyrophyllite was studied in many deposits around the world [1-4, 8-10] (Table 1). However, the pyrophyllite ore genesis in the Ougnat inlier has not been extensively studied. [11, 12] have focused on the position of the host-rocks of pyrophyllite within the Proterozoic history. The works of [13, 14] showed that the pyrophyllite of the Ougnat inlier correspond to a fracture network that played as N150° corridors of Neoproterozoic ductile shear zones. The pyrophyllite development is then penecontemporaneous with the shearing [14]. In this work, we try to show the relationship between the Neoproterozoic volcanic rocks (the Ouarzazate group) of the Ougnat inlier and the pyrophyllite deposits. In this context, we present the field observations, the mineralogical and textural arguments in favor of the metasomatic origin of these pyrophyllite concentrations.

It should be noted that, in addition to these two studied deposits selected for the easing access to ore bodies at different levels offered by the exploitation, other indices outcrop within the Ougnat Precambrian inlier. Despite their dark patina, these concentrations of pyrophyllite are recognizable by their soft rheology and their phyllitic or massive appearance, and especially by their light color of fresh fracture, clearly contrasting with the original volcanic protolith.

2. Geological setting of the Ougnat inlier

Moroccan Anti-Atlas is located on the northern edge of the West African Craton (WAC). With ENE-WSW orientation, it extends from the southern edge of the High Atlas in the north, to the north side of the Carboniferous Basin of Tindouf at the south. The Souss, Ouarzazate and Errachidia-Boudenib basins separate it from the High Atlas belt. The Anti-Atlas has an elongated shape; it is composed by Paleozoic cover overlying old Precambrian rocks, and giving a string of inliers that mark the centerline of the Anti-Atlas. From the WSW to the ENE, the most important Precambrian inliers are: Bas-Drâa, Ifni, Kerdous, Irherm, Sirwa, Zenaga, Bou-Azzer, Saghro and Ougnat.

Table 1: Comparison of composition of pyrophyllite from different locations. Ougnat deposit: analyses performed by [14] and other deposits: data synthesized from different works by [39].

| | Ougnat | South Africa | Sweden | North Carlina | Californie | Japon | New Zeland |
|------------------------------------|--------|--------------|--------|---------------|------------|--------|------------|
| SiO₂ (wt. %) | 67.14 | 57.26 | 64.88 | 66.04 | 65.96 | 63.57 | 62.70 |
| TiO₂ | 0.01 | 1.76 | 0.02 | 0.00 | tr | 0.04 | 0.00 |
| Al₂O₃ | 27.90 | 31.03 | 28.64 | 28.25 | 28.25 | 29.25 | 29.70 |
| Fe₂O₃ | 0.12 | 1.58 | 0.48 | 0.64 | 0.18 | 0.22 | 1.00 |
| MnO | 0.04 | 0.01 | 0.02 | 0.02 | 0.00 | 0.00 | 0.00 |
| MgO | 0.03 | 0.00 | 0.08 | 0.06 | 0.00 | 0.37 | 0.00 |
| CaO | 0.05 | 0.00 | 0.03 | 0.06 | 0.00 | 0.38 | 0.00 |
| Na₂O | 0.10 | 0.00 | 0.03 | 0.03 | 0.00 | tr | 0.20 |
| K₂O | 0.02 | 1.43 | 0.04 | 0.03 | 0.00 | 0.02 | 0.00 |
| P₂O₅ | 0.05 | 0.11 | 0.00 | 0.00 | 0.00 | 0.00 | 0.00 |
| Volatiles | 4.56 | 6.23 | 5.56 | 5.02 | 5.41 | 6.32 | 6.40 |
| Total | 100.02 | 99.41 | 99.78 | 100.15 | 99.8 | 100.17 | 100 |

The Jbel Ougnat is the easternmost inlier of the Anti-Atlas. In this area, the Pan-African Anti-Atlas is linked up with the Ougarta (Figure 1A). The Ougnat inlier is bounded north by the South Atlasic Furrow, east by the Tafilalt plain, south by the Maïder plain and west by the Jbel Saghro. Ougnat and Saghro both constitute the Eastern Anti-Atlas.

Geological studies of the Moroccan Anti-Atlas have started since the beginning of the last century with the works of [13, 15-20]. They were followed by publishing a number of geological maps, latest ones are the maps 1/50 000th of the National Plan for Geological Mapping (PNCG for "Plan National de la Cartographie Géologique") launched in 1996 by the Moroccan Ministry of Energy, Mines, Water and Environment (Maps of: Oukhite, Bou Adil, Marzouga, Irara, Al Atrous, Mfis and Tawz). Recent geological studies were also performed in Jbel Ougnat such as [21-26] ...

The Jbel Ougnat inlier consists of a folded metasedimentary Neoproterozoic basement (Saghro Group). U-Pb detrital zircon dating suggest 610-620 Ma as maximum age of sedimentation of the Saghro Group greywackes next of Bou Salda Formation [27]. The U-Pb zircon dating showed that the Saghro Group is intruded lately by the 547±26 Ma-old Mellab granodiorite [28] (Figure 2B). A volcano-sedimentary cover of the terminal Neoproterozoic (Upper Ediacarian) unconformably overlies the whole. Paleozoic sedimentary rocks (Figure 2B) surmount this sub-tabular cover.

The anticlinal structure of the Jbel Ougnat inlier shows the Neoproterozoic at the center and Paleozoic cover in the borders (Figure 2B). With a varied lithology, the bedrock shows a multiphase geological activity, which explains its complexity. The Neoproterozoic consists of two major geological domains:

- ✓ Neoproterozoic metasedimentary basement: this serie is comparable to Neoproterozoic series described in Imiter and Kelaa M'Gouna inliers respectively by [30] and [31]. The Saghro Group bedrock, where metagreywackes are deformed, schistosed and metamorphosed in greenschist facies with chlorite and sericite [11, 18] and granitized at the Pan-African Orogeny. These terrains outcrops in the north central of the Ougnat inlier, in center of the Ougnat anticline. Granitoids shows two different petrographic facies; (i) quartz diorite and (ii) garnet-granite [32]. The implementation of the two granitoids is supposed synchronous [13] and [32]. These intrusions developed a biotite, cordierite, andalusite and garnet contact metamorphism in the metasedimentary series. Relations between the granitoids and the folding of the sedimentary series show that the Eastern Anti-Atlas granitoids are tardi-tectonics to post-tectonics [33].
- ✓ Terminal Neoproterozoic volcano-sedimentary cover: this serie is formed by volcanic and volcanosedimentary rocks of the Ouarzazate Group (Ediacaran); the geological formation enclosing

mineralization of pyrophyllite, subject of this study. This cover consists from bottom to top: (i) conglomerates with angular and heterometric elements that formed by products of dismantling the metasedimentary series and granitoids. It corresponds to chaotic accumulations along N30° major fractures [34]. (ii) The Tamerzaga Formation composed by a stack of ignimbric plies and intercalated andesite lava flow. (iii) The Ouin Oufroukh Formation, which includes sedimentary and volcano-sedimentary rocks (limestone, cherts, mudstone, sandstone, conglomerates), tuffs and rhyolites and andesites levels. (iv) The Aoujane Aïssa Formation is dominated by ignimbric rocks with some intercalations of dacitic and basaltic lava flow [35] (Figure 3A). It ends with the establishment of the only basaltic lava flow in the region. However, recent work of [24] modified the lithostratigraphic column of [35]. He subdivided the Terminal Neoproterozoic into three principal formations: Tamerzaga, Bou Naga and Aoujane Aïssa formations separated by two volcano-sedimentary intercalations, and many plutonic intrusions (mainly granodiorite).

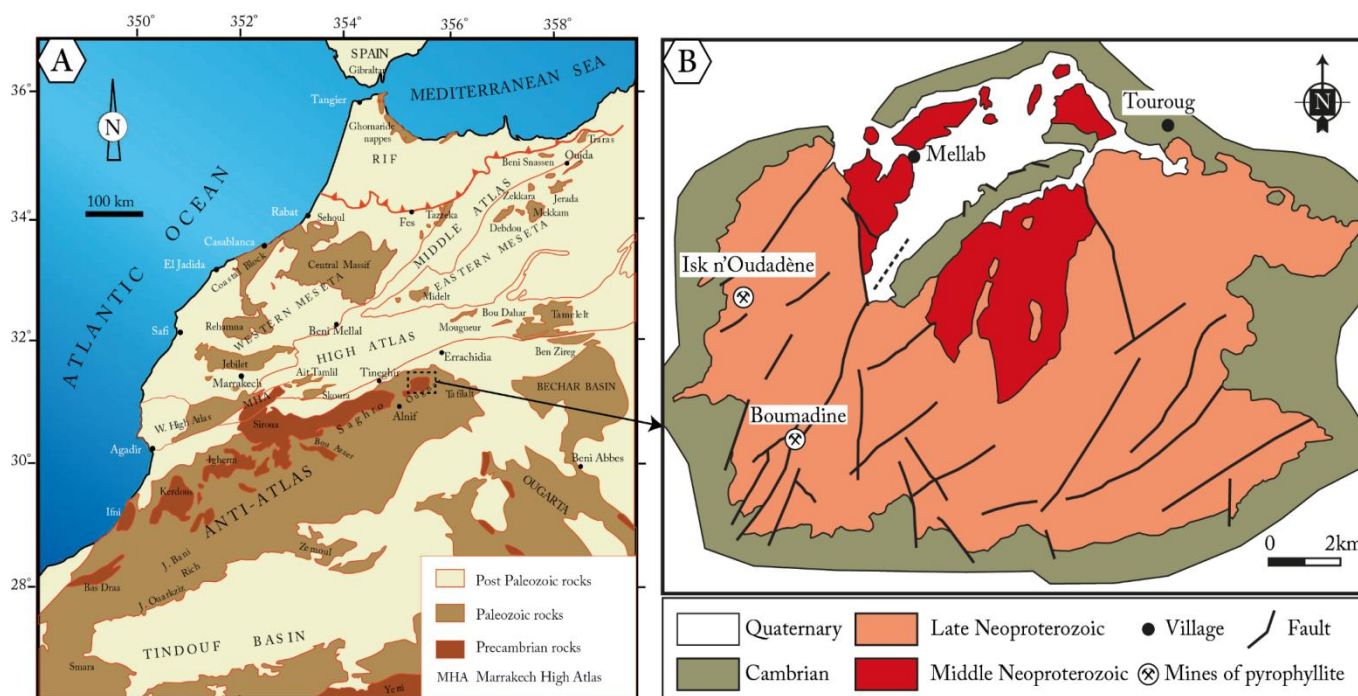


Figure 2: (A) Extension of the Paleozoic and Precambrian outcrops in Morocco (Northern Provinces) and westernmost Algeria (Traras, Ben Zireg, Béchar) [29] and (B) Simplified geological map of the Jbel Ougnat inlier [20].

Concerning the Paleozoic cover in the Jbel Ougnat inlier, the Paleozoic transgression gradually extends from the SW to the NE of the eastern Anti-Atlas during the Lower Cambrian [36, 37]. The Cambrian series contain sandstone and pelites terms (Pardoxide shale, "Schistes à Paradoxides") and sandstone (Tabanit sandstone, "Grès de Tabanit") in which large alkali basalt formations are intercalated. Paleozoic series continues in this region by Ordovician to Lower Carboniferous terms in the south and the east of the Ougnat inlier, totaling approximately 4 km-thick [22] (Figure 3).

Concerning the Paleozoic cover in the Jbel Ougnat inlier, the Paleozoic transgression gradually extends from the SW to the NE of the eastern Anti-Atlas during the Lower Cambrian [36, 37]. The Cambrian series contain sandstone and pelites terms (Pardoxide shale, "Schistes à Paradoxides") and sandstone (Tabanit sandstone, "Grès de Tabanit") in which large alkali basalt formations are intercalated. Paleozoic series continues in this region by Ordovician to Lower Carboniferous terms in the south and the east of the Ougnat inlier, totaling approximately 4 km-thick [22] (Figure 3).

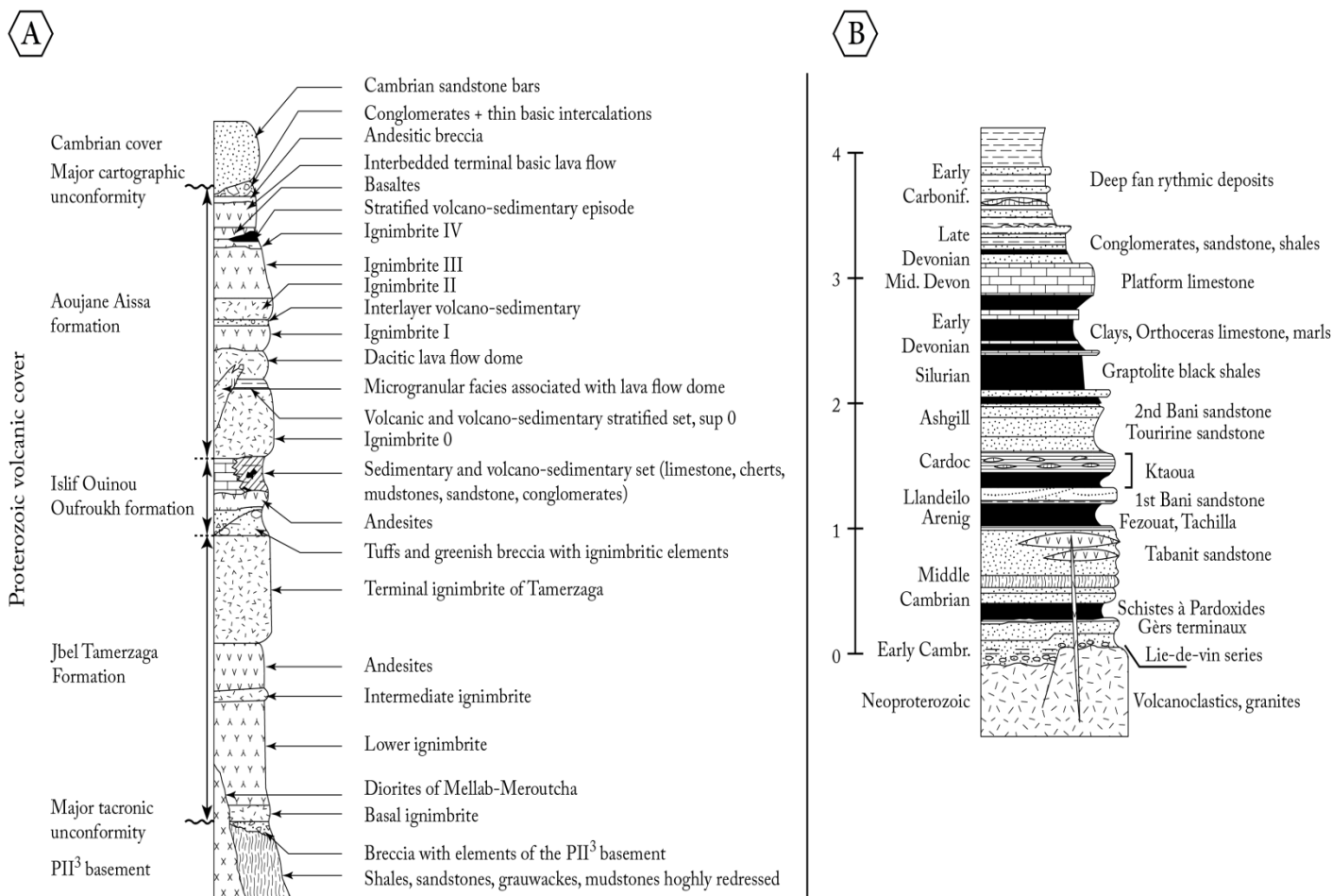


Figure 3: Synthetic stratigraphic columns of the Eastern Anti-Atlas: **(A)** Neoproterozoic of the Central Ougnat [35] and **(B)** Paleozoic formations, synthesized by [22].

3. Methodology

Although pyrophyllite indices and deposits are numerous in the Jbel Ougnat, we focused our study on the Isk n'Oudadène and Boumadine deposits (respective GPS coordinates: 31.47°N, 4.95°W and 31.39°N, 4.92°W). The open-pit mining work carried out on these deposits gives a double advantage: they allowed to (i) access to the pyrophyllite ore bodies in different levels and (ii) carry out a systematic sampling from the protore (acid volcanic rocks) to the most advanced pyrophyllite (representing a maximum transformation of the original rock). We have carried out several macroscopic observations of the mineralogical and textural evolution of the pyrophyllite at different levels, and microscopic observations using a petrographic microscope (transmitted light mode). Polished thin sections have been observed using an Olympus BX41 microscope associated with Olympus camera (E-330 model). These observations allowed us to follow the mineralogical and textural changes.

4. Results and discussion

4.1. Macroscopic study

At outcrop scale, in the open pit mine, there is a gradual evolution of color, rheology and appearance of the rock (phyllitic or massive). Indeed, going from the volcanic protolith to the most advanced pyrophyllite, the color is increasingly clear, the rock is progressively softer and takes a massive or phyllitic appearance (Figure 4). This trend appears clearly on both patina and fresh fracture.



Figure 4: Pyrophyllite outcrop in the Boumadine open pit mine illustrating color changes and consequently pyrophyllite petrology evolution from the periphery to the center of the deposit.

In order to refine our outcrop observations, samples used for the thin sections preparation coming from different levels of pyrophyllite were macroscopically observed. The observation reveals color contrast that progressively advance from the dark pole (acid volcanic protolith) to clear pole (advanced pyrophyllite) (Figure 5).

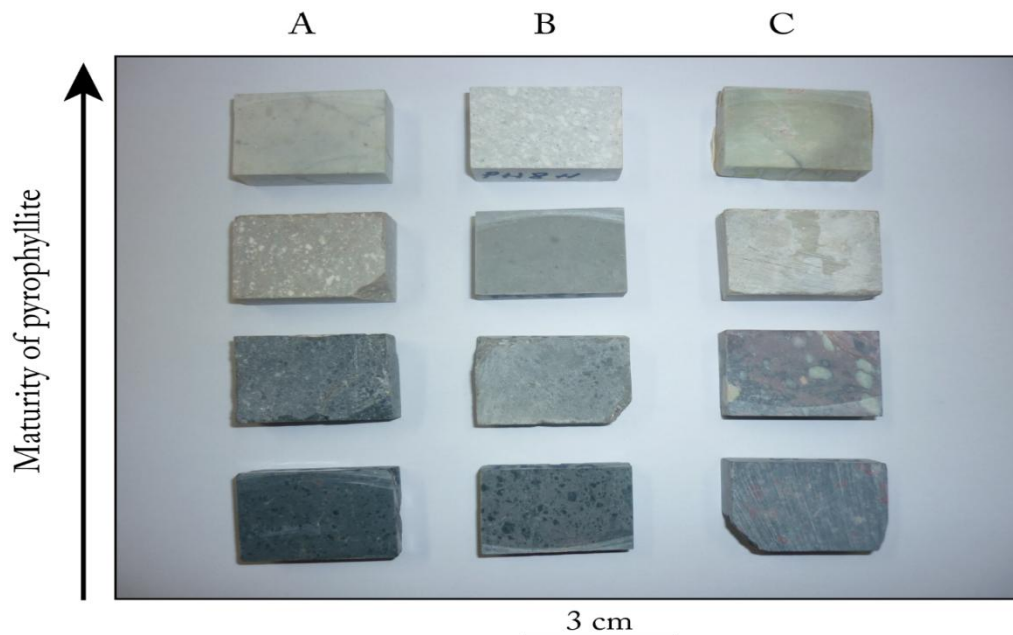


Figure 5: Color evolution on fresh fracture of pyrophyllite in the two main studied deposits (A and B: Isk n'Oudadène, C: Boumadine).

4.2. Mineralogical and textural study

The gradual evolution of the pyrophyllite color is certainly the result of a transformation process that acts on the original rock and changes its chemistry, mineralogy and texture. To highlight this phenomenon and the nature of the transformations occurred, the observation of thin sections made at different levels of the two deposits Isk n'Oudadène and Boumadine was made. Thus, we observed that:

In the protolith, the quartz appears with embayments (or 'corroded' margins) (Figure 6A and 6B) characteristic of rhyolitic volcanic rocks. After pyrophyllitization, this quartz becomes a mineral with indented edges and shows transformation halos (Figures 6D, 6E and 6F). Micro-flakes of pyrophyllite appear glued to the corroded quartz contours (Figure 6E). Some quartz crystals are completely disintegrated into scattered pieces (Figure 6E). These have the same extinction in polarized light indicating an identical orientation of their ellipsoids indices, and therefore demonstrating that these small pieces of quartz derived from a same primary quartz crystal whose the external shape is preserved (Figure 6D, 6E and 8A).

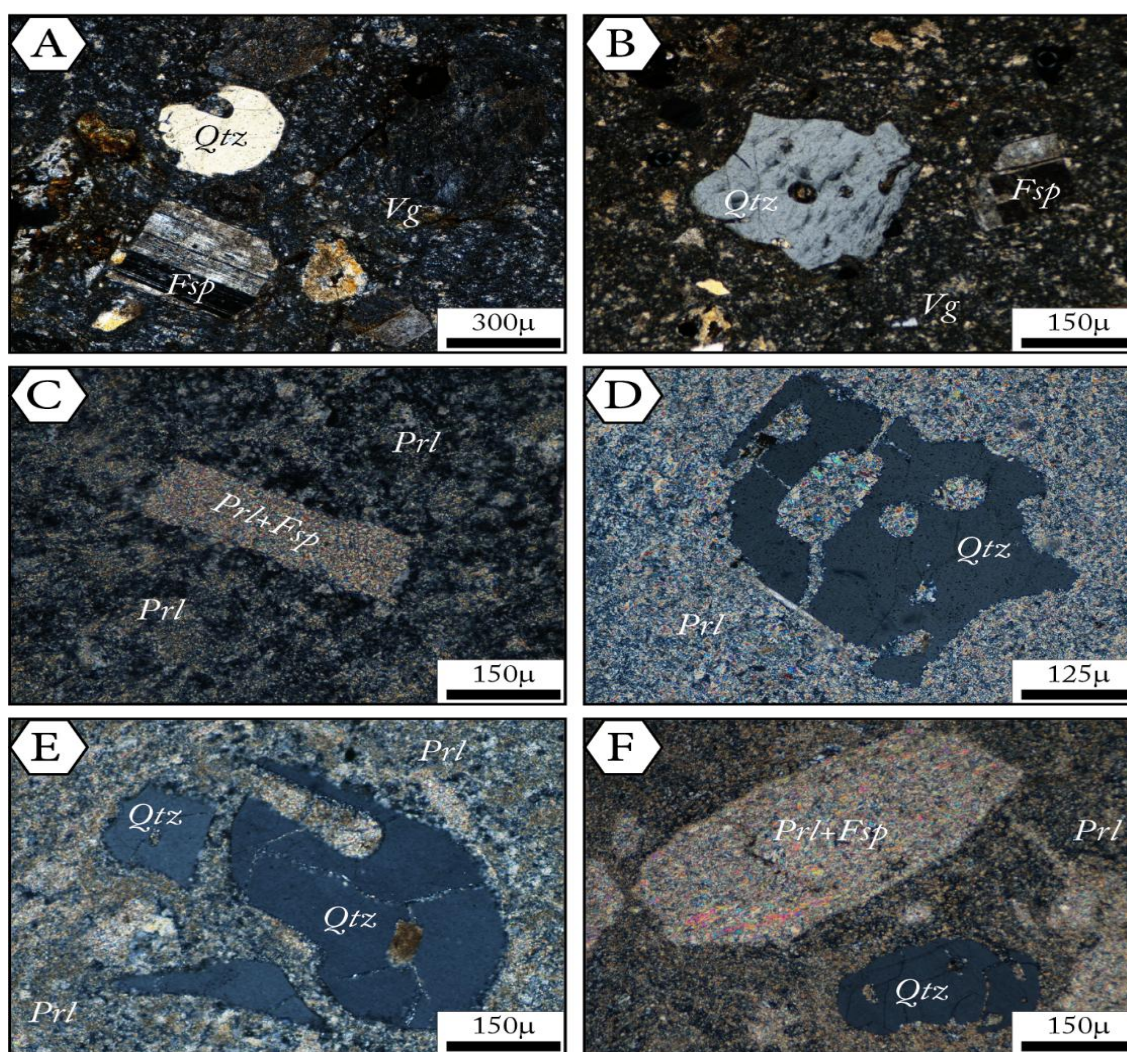


Figure 6: Photomicrographs of thin sections derived from different levels of mineralization. (A) and (B) rhyolitic protolith with quartz, feldspar and volcanic glass (TL, nic.+). (C) total pyrophyllitization of feldspar with conservation of its original shape (TL, nic.+). (D) partial pyrophyllitization of quartz, note the uniform extinction of all parts of the quartz in (D) (TL, nic.+). (E) crystal of quartz disintegrated into scattered pieces. (F) total transformation of feldspar to pyrophyllite and partial pyrophyllitization of quartz indicating that quartz is more resistant to alteration compared to feldspar (TL, nic.+). Fsp: feldspar, Qtz: quartz, Prl: pyrophyllite, TL: transmitted light, nic. +: crossed nicols.

Alkali feldspars and plagioclases, initially intact at the original volcanic rock (Figure 6A and 6B), are firstly partially transformed (Figure 6C), and in an advanced stage of pyrophyllitization, they are totally transformed to pyrophyllite (Figure 6F and 8B). The transformation occurred while keeping the first shape of the primary mineral. When the pyrophyllitization reached a paroxysmal stage, the feldspar phenocrysts are homogenized with the mesostase initially microcrystalline and vitreous, to give a homogeneous massive dough of pyrophyllite (micro-flakes of pyrophyllite) (Figure 8C).

In partially or completely pyrophyllitized facies, we recognize the phantoms of ferromagnesian minerals. We distinguish:

- ✓ Hornblende crystals, which are recognizable by the shape of their basal section and their double-cleavage forming angle of about 60° . This double-cleavage is enhanced by iron oxides (Figure 7A). Figure 7C shows a longitudinal section of the hornblende with single cleavage plane;
- ✓ Biotite with single cleavage plane on its longitudinal section (Figure 7B) characteristic of the species;

The common factor between all ferromagnesian minerals is that their interiors are partially or totally substituted by pyrophyllite and iron oxides (Figures 7A, 7B and 7C). The maturity stage of pyrophyllite depends on the sample position in the series (position relative to protolith), and therefore the evolution state of its pyrophyllitization.

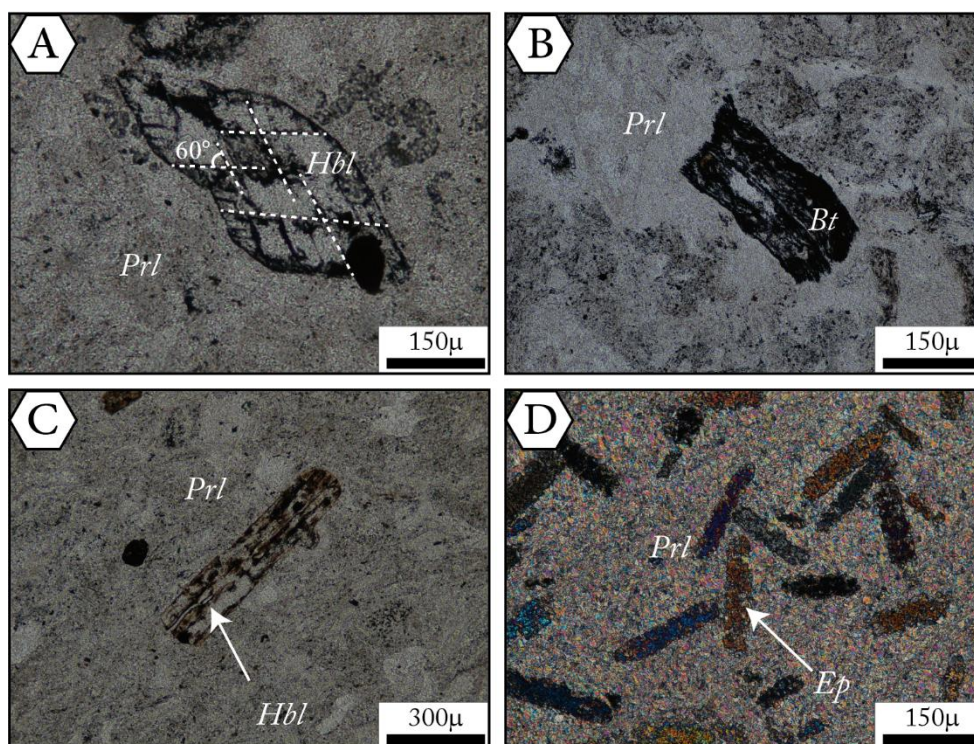


Figure 7: Photomicrographs of thin sections derived from different levels of mineralization. (A) phantom of hornblende basal section, where cleavage filled with iron oxides, draw a 60° angle (TL, nic. //). (B) biotite crystal in pyrophyllitized volcanic glass (TL, nic. //). (C) phantom of longitudinal section of hornblende in pyrophyllitized volcanic glass (TL, nic.//). (D) epidote crystals in pyrophyllitized volcanic glass (TL, nic. +). Bt: biotite, Ep: epidote, Hbl: hornblende, Prl: pyrophyllite, TL: transmitted light, nic. //: parallel nicols, nic. +: crossed nicols.

In some pyrophyllite ore locations, there is an association between epidote and micro-flakes of pyrophyllite. These two minerals continue to inter-react after formation of epidote subautomorphic crystals. Consequently, we obtain epidote minerals with gnawed edges, indicating that epidote finished growing before achievement of pyrophyllitization phenomenon (Figure 7D).

From a textural point of view, the macroscopic and microscopic observations of the different samples allowed us to notice that:

- ✓ From the protolith to the most advanced pyrophyllite in each ore deposit (Isk n'Oudadène and Boumadine), we distinguish a number of mineralogical transformations. So, we move from a porphyritic texture with phenocrysts of quartz and feldspar (Figures 6A and 6B), to a rock reflecting an intermediate degree of transformation characterized by corroded quartz and phantoms of feldspar (Figures 6D, 6E, 6F, 8A and 8B). The mesostase is partially pyrophyllitized and contains remains of quartz crystals and small-scattered opaque grains (iron oxides, Figures 7A and 7B).
- ✓ From the initial porphyritic texture, solely quartz grains persist and shows disaggregated into smaller flakes and have severely indented edges. When pyrophyllitization reach a final stage, the original texture is then almost completely erased (Figure 8C). The residual quartz is explained by the fact that this mineral is more resistant to alteration compared to feldspars and ferromagnesian minerals.
- ✓ In addition to pyrophyllite deriving from minerals and volcanic glass transformation, some veins filling pyrophyllite flakes and limpid neogenic quartz were also observed; particularly in partially transformed rocks (Figure 8D). The mineralizing fluid therefore reacts with the protolith rock to precipitate pyrophyllite in fractures.

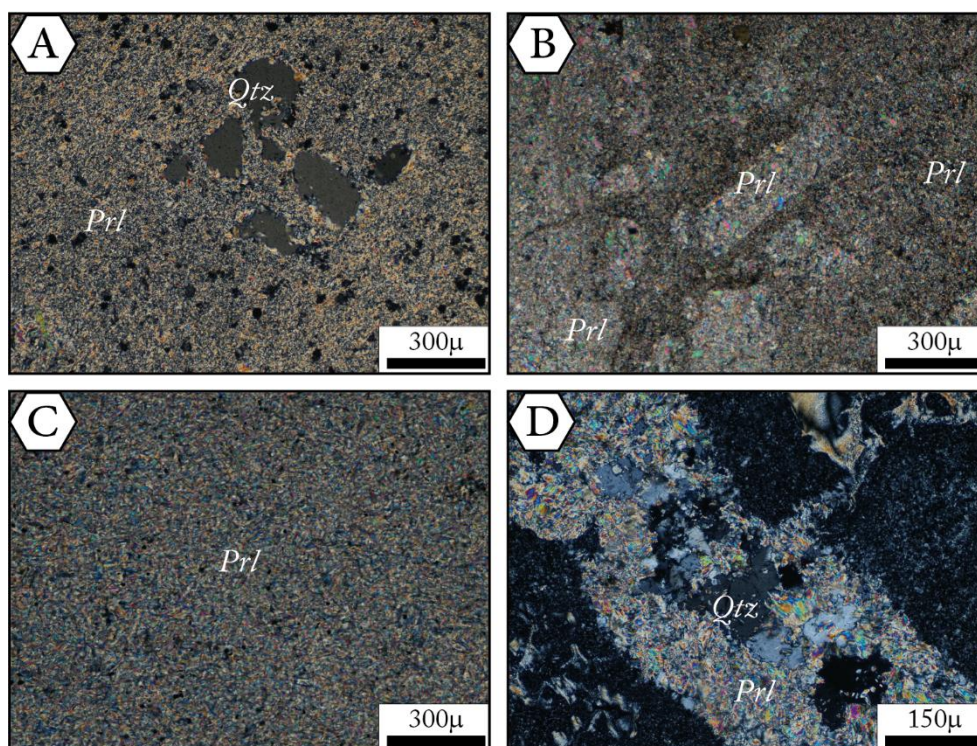


Figure 8: Photomicrographs of thin sections derived from different levels of mineralization. (A) Several pieces of the same quartz crystal in pyrophyllite. Note the indented edges of quartz (TL, nic.+). (B) advanced stage of feldspar pyrophyllitization. These ones are completely transformed but they keep the original shape (TL, nic.+). (C) paroxysmal stage of pyrophyllitization where all component of the original volcanic rock are homogenized (quartz, feldspar, ferromagnesian minerals and volcanic glass) (TL, nic.+). (D) neogenic limpid quartz and pyrophyllite in microfractures (TL, nic.+). Qtz: quartz, Prl: pyrophyllite, TL: transmitted light, Nic. +: crossed nicols.

4.3. Discussion of the results

Previous observations (macroscopic and microscopic) show that pyrophyllite ores derived from rhyolitic rocks. It obvious that pyrophyllitization of these volcanic rocks is more important in the centers of the deposits than in their peripheries. According to experimental work [38], the pyrophyllitization of the rhyolitic rocks may have

proceeded in several stages. [2] and lately [3] describe progressive alteration of rhyolite. They consider the fluid responsible for pyrophyllitization of the rhyolitic rocks in the Foxtrap deposit was most likely derived from the adjacent Holyrood pluton probably during or shortly after its intrusion. After [3], this fluid may have been significantly enriched in components such as HCl and KCl. Dissociation of these components would occur on cooling and providing the driving mechanism for the intense hydrothermal alteration which ultimately resulted in the complete pyrophyllitization of the fractured and sheared rhyolites. This situation appears to be the same in our studied deposits where pyrophyllitization is controlled by N150° corridors developed in a shear zone [14]. The composition of the fluid will progressively change. The early (high-temperature) stages of the fluid will precipitate pyrophyllite, whereas the later (lower temperature) stages will give intermediate mineralogical phases. On another side, [5] concluded that in Pinite mine in Nevada, the granodiorite intruded into the region during the Jurassic, provided the mineralizing fluids which both generated the silicification of the Weaver Rhyolite and the subsequent hydrothermal metasomatism, which replaced the silicified volcanics with sericite and pyrophyllite. Finally, in our study, mineralizing fluid is probably derived from the near Mellab granitoids.

Concerning the physical conditions of pyrophyllite formation (pressure and temperature), [2] showed that the alteration of the rhyolite of Newfoundland took place in pressure of 2 kbar and a temperature range of approximately 260-280°C, and that the temperature very likely did not exceed 300°C. In addition, [1] concluded that the Newfoundland pyrophyllite deposits were formed by the metasomatic replacement of previously silicified rhyolites by thermal waters under conditions involving dynamic stress and intermediate temperatures and pressures. The solutions evidently moved along fault or shear zones.

We note that microprobe analyses performed by [14] show that the monoclinic pyrophyllite of the Ougnat inlier (Isk n'Oudadène and Boumadine deposits) show a similitude with another pyrophyllite deposits in Sweden, North Carolina, California Japan and New Zeland, but different from pyrophyllite of the Republic of South Africa [39] (Table 1).

All these previous results obtained on other pyrophyllite deposits are reliable with our studied deposits. Using these results accompanied by our field and microscopic observations, we can conclude also that pyrophyllite of Isk n'Oudadène and Boumadine is obtained by metasomatic alteration of terminal Neoproterozoic rhyolite.

5. Conclusion

Present study concerned pyrophyllite of two great ores in the Eastern Anti-Atlas. Both mineralogical and textural observations allow us to conclude that pyrophyllitic concentration derives from rhyolitic rocks by a metasomatic phenomenon. Mineralizing fluid is responsible for alteration of primary acidic volcanic rocks (rhyolite) to precipitate pyrophyllite concentrations. The pyrophyllitization degree is increasing from peripheries of the rhyolite to the most "mature" pyrophyllite. Therefore, in the intact protolith, we find feldspar, ferromagnesian, corroded quartz and volcanic glass, whereas in an intermediate stage of pyrophyllitization, these minerals disappear leaving only their phantoms. When pyrophyllitization process reached a paroxysmal stage, all components of the rhyolite are transformed to pyrophyllite and provide a homogeneous facies of pyrophyllite. We cannot distinguish either the primary minerals or their original shape.

Acknowledgments - We thank the companies Zenaga and Ouisselsate-Mine for providing access to the two studied mines. We also indebted to I. Assoussi for the thin sections preparation. We also express our gratitude to E. M. Mouguina and M. Ikkene for their comments that significantly improve the manuscript. Thanks also to A. Ali Ammar for English revision.

References

1. Buddington A.F., *J. Geol.*, 24 (1916) 130-152.
2. Papezik V.S., Keats H.F., *Can. Mineral.*, 14 (1976) 442-449.
3. Bryndzia L.T., *Econ. Geol.*, 83 (1988) 450-453.
4. Hayes J.P., *Mem. Univ. of Newfoundland*, (1996) 189.

5. Crouse D.L., Embree P., *Ariz. Geol Surv., Spec. Paper*, (2014) 1-8.
6. Ciullo P.A., Thompson C.S., *Soc.Min., Metall., Explor.*, (1994) 815-826.
7. Jébrak M., Marcoux É., *Minist. ress. nat. faune*, (2008), 685p.
8. Gruner J.W., *Zeitschrift her Kristallographie*, 88 (1934) 412.
9. Hendricks S.B., *Zeitschrift her Kristallographie*, 99 (1938) 264.
10. Henriques H., *Arkiv foer Mineralogi och Geologi*, 2 (1957) 279.
11. Lécolle M., Derré C., Hadri M., *Afr. Geo. Rev.*, 10 (2003) 227-244.
12. Lécolle M., Derré C., Hadri M., *Min., Géol. Ener.*, 52 (2003) 45-68.
13. Abia E.H., *Univ. Ibno Zohr, Agadir*, (2001) 244.
14. Abia E.H., Ibhi A., Nachit H., Nouidir M., *Coll. Magm. Métam.Minér. Ass.*, (2005) 1-3.
15. Gentil L., *F. Alcan.*, (1912) 319.
16. Bourcart J., *Bull. Soc. Géol. Fr.*, (4) 27 (1927) 10–11.
17. Neltner L., *C. R. Acad. Sci. Paris*, 188 (1929) 871–873.
18. Lécolle M., Derré C., Nerci K., *Ore Geol. Rev.*, 6 (1991) 501-536.
19. Abia E.H., *Univ. Cadi Ayad*, (1991) 184.
20. Abia E.H., Nachit H., Marignac C., Ibhi A., Saadi S.d.A., *J. Afr.Earth Sci.*, 36 (2003) 251-271.
21. Baidder L., *Univ. Hassan II Casablanca*, (2007).
22. Raddi Y., Baidder L., Tahiri M., Michard A., *Bull. Soc. Géol. Fr.*, 178 (2007) 343-352.
23. Baidder L., Raddi Y., Tahiri M., Michard A., *Geol. Soc. London, Spec. Pub.*, 297 (2008) 453-465.
24. Raddi Y., *Univ. Mohamed V, Rabat*, (2014) 313.
25. Soulaïmani A., Michard A., Ouanaimi H., Baidder L., Raddi Y., Saddiqi O., Rjimati E.C., *J. Afr.Earth Sci.*, 98 (2014) 94-112.
26. Baidder L., Michard A., Soulaïmani A., Fekkak A., Eddebbi A., Rjimati E.C., Raddi Y., *J. Afr.Earth Sci.*, 119 (2016) 204-225.
27. Abati J., Aghzer A.M., Gerdes A., Ennih N., *Precambrian Res.*, 181 (2010) 115-128.
28. Mrini Z., *Univ. Cadi Ayyad, Marrakech*, (1993) 227.
29. Michard A., Frizon de Lamotte D., Saddiqi O., Chalouan A., *Spring. Berl. Heidelberg*, (2008) 1-31.
30. Marini F., Ouguir H., *C.R. Acad. Sci. Paris*, 310 (1990) 577-582.
31. Fekkak A., Boualoul M., Badra L., Amenzou M., Saquaque A., El-Amrani I.E., *J. Afr.Earth Sci.*, 30 (2000) 295-311.
32. El Baghdadi M., El Boukhari A., Jouider A., Benyoucef A., Nadem S., *Pangea*, 35/36 (2001) 5-26.
33. Errami E., Bonin B., Laduron D., Lasri L., *J. Afr.Earth Sci.*, 55 (2009) 105-124.
34. Ait Saadi S., *Instit. Polytech. Lorraine*, (1992) 214.
35. Paile Y., *Paris XI, Orsay, France*, (1983) 290.
36. Du Dresnay R., Hindermeier J., Emberger A., Caïa J., Destombes J., Hollard H., *Notes Mém. Serv. Géol. Maroc*, 243 (1988)
37. Destombes J., *Notes Mém. Serv. Géol. Maroc*, (2006)
38. Tsuzuki Y., Mizutani S., *Contrib. Mineral. Petr.*, 30 (1971) 15-33.
39. Hicks T.L., Secco R.A., *Can. J. Earth Sci.*, 34 (1997) 875-882.

(2017) ; <http://www.jmaterenvirosci.com/>